MRS Communications (2019), 9, 203–208
© Materials Research Society, 2019
doi:10.1557/mrc.2019.2

MRS Communications

Research Letter

Thermal stability of two-dimensional titanium carbides $Ti_{n+1}C_n$ (MXenes) from classical molecular dynamics simulations

Vadym Borysiuk, Sumy State University, 40007 Sumy, Ukraine
Vadym N. Mochalin, Department of Chemistry and Department of Materials Science and Engineering, Missouri University of Science and Technology, Rolla, Missouri 65409, USA

Address all correspondence to Vadym N. Mochalin at **mochalinv@mst.edu**

(Received 23 September 2018; accepted 4 January 2019)

Abstract

We report the classical molecular dynamics (MD) study of thermal stability of three two-dimensional (2D) titanium carbides Ti_2C, Ti_3C_2, and Ti_4C_3 (MXenes). Thermal properties of 2D nanomaterials are of fundamental importance and raise particular interest due to their potential applications in nanoelectronics. To investigate the behavior of $Ti_{n+1}C_n$ MXenes during heating, structural parameters such as Lindemann indexes, radial distribution functions, and atomistic configurations were calculated. The analysis of MD data allowed us to obtain approximate values of MXene degradation temperatures that are 1050, 1500, and 1700 K for Ti_2C, Ti_3C_2, and Ti_3C_4 MXenes, respectively.

Introduction

Thermal stability is one of the most important attributes of any material used in manufacturing of electronic devices. Thermal stability is even more important in various nanotechnologies, as the nanomaterials are typically characterized by lower melting points compared to their counterpart bulk materials.[1,2]

Two-dimensional (2D) titanium carbides $Ti_{n+1}C_n$ are relatively new nanomaterials that belong to a large family of MXenes—transition metal carbides and nitrides with a thickness from 3 atomic layers and more.[3] Recent studies have revealed extraordinary electrical and electrochemical properties of MXenes, which, together with their unique 2D structure and hydrophilicity make them promising materials for supercapacitors, Li and beyond lithium batteries, hydrogen storage, optical and THz applications[4,5] and environment sensing,[6] triboelectric energy generation and harvesting, etc.[7–12] Besides this, due to their high mechanical properties, namely high Young's modulus[13–16] and bending rigidity exceeding that of monoatomic layer materials such as graphene or hexagonal boron nitride,[14,17] MXenes are advantageous for applications in composites, sensors, and resonators where high frequency of vibrations is required. Thus, the investigation of thermal properties and determination of the range of temperatures where MXenes preserve their 2D structure is an important task.

Experimental studies of thermal stability of Ti_2C and Ti_3C_2 MXenes are presented in Refs. 18 and 19, where authors studied thermal stability, phase transformations, and oxidation of MXenes terminated with F and OH surface functional groups during heating under oxygen and argon atmospheres. According to Ref. 19 Ti_3C_2 MXene with F/OH surface terminations is stable under argon atmosphere at temperatures up to 800°C. At the same time, the authors reported that at 200°C under oxygen atmosphere MXene was partially oxidized forming anatase nano-crystals distributed on Ti_3C_2 layers. At 1000°C under oxygen atmosphere, complete oxidation of MXene layers and transformation of anatase phase to rutile were observed. Experimental studies of Ti_2C MXene reported in Ref. 18 show the formation of anatase TiO_2 on Ti_2C MXene at lower temperature (500 K), followed by transformation to rutile at higher temperatures.

However, no data on thermal stability of pristine bare $Ti_{n+1}C_n$ MXenes with exact determination of the temperature stability range were reported so far.

In this paper we present an *in silico* study of the thermal behavior of three $Ti_{n+1}C_n$ MXenes with $n = 1, 2, 3$ using classical molecular dynamics (MD) simulations. MD simulations are widely used for investigation of thermal behavior of various nanomaterials such as metallic nanoparticles,[2,20] carbon nanotubes,[21] and 2D crystals[22,23] as they provide unique atomistic level insights into the melting processes that occur at the nanoscale.

Until recently, the main problem with classical MD simulations of MXenes was the absence of the reliable forcefield that would accurately reproduce interactions between the atoms of elements typically found in MXenes (e.g., Ti, C, O, H, F). Recent parameterization of the Reactive Force Field (ReaxFF)[24–26] now allows precise description of chemical bonding in MXenes, however ReaxFF is quite complex, and thus modeling of large samples requires significant investments in computational power. In the proposed study we used a

https://doi.org/10.1557/mrc.2019.2 Published online by Cambridge University Press

simpler approach formulated in Refs. 15 and 17 based on the combination of interatomic potentials, which allows inexpensive large-scale MD simulations of $Ti_{n+1}C_n$ MXenes. To detect the phase changes and estimate the range of thermal stability of the samples, quantitative structural parameters such as Lindeman indexes[21] were calculated in the considered range of temperatures. To validate obtained data, the temperature dependencies of the potential energies and radial distribution functions (RDF) were also computed.

It is worth mentioning that oxidation of Ti_3C_2 MXene with surface groups at various temperatures and in different environments was recently studied by ReaxFF MD simulation,[26] which allows for formation and breaking of chemical bonds accompanying chemical and physical transformations in the system. Within our simulations we did not consider phase transformations and formation of new compounds during heating, as our aim was to detect the range of temperatures within which the $Ti_{n+1}C_n$ samples preserve their 2D sheet-like structure. Even though we used simple MD approach, our study provides new data that may become a useful first-order approximation for further investigations of thermodynamic properties of MXenes and for the design of novel electrical and mechanical devices incorporating these 2D materials.

Simulation setup

We consider rectangular $Ti_{n+1}C_n$ nanosheets with $n = 1$, 2, 3 and lateral size 20×17 nm in a Cartesian coordinate box with periodic boundary conditions in the xy direction and free boundary condition in the z direction. An example typical configuration of the system is shown in Fig. 1 (all MD snapshots in this paper were produced using Visual Molecular Dynamics software[27]). Previously developed in-house code for parallel computing was employed to calculate the interatomic forces between atoms in the samples during heating. Detailed description of the developed approach and corresponding interatomic potentials can be found in Refs. [15,17] and [28,29], respectively.

Heating of the $Ti_{n+1}C_n$ nanosheets was simulated by increasing temperature using Berendsen thermostat,[30] according to the scheme described in Ref. 2. Temperature of the samples was increased from the initial value of 300 K in 50 K increments. Similar to Ref. 2, at each particular temperature the system was simulated for 100,000 MD steps (≈ 20 ps), during which all data required for calculation of the structural parameters were recorded. Then the temperature was increased to the next value and the procedure repeated. Around the thermal degradation point the temperature increment was reduced to 10 K for a better accuracy.

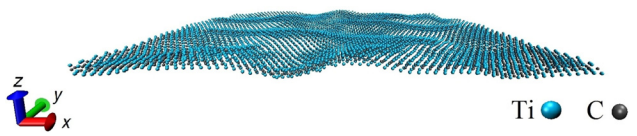


Figure 1. Typical configuration of Ti_2C nanosheet at $T = 300$ K used in this study.

To characterize MXene stability and thermal degradation we calculated the Lindeman indexes. Lindemann index is a commonly used parameter in MD simulations of melting processes. It indicates changes in crystal structure of the sample due to thermal disorder. The local Lindemann index q_i of an atom i is defined as[21]:

$$q_i = \frac{1}{N-1}\sum_{j\neq i}\frac{\sqrt{\langle r_{ij}^2\rangle - \langle r_{ij}\rangle^2}}{\langle r_{ij}\rangle}, \quad (1)$$

where r_{ij} is a distance between atoms i and j, and angle brackets indicate time average at constant temperature. Lindemann index q of a sample consisting of N atoms can be estimated by averaging over all atoms in the system.

The melting point of the sample can be determined from the critical value of the Lindeman index q_c. The range of values $q_c \approx 0.1$–0.15 is typically used as a melting criterion for bulk solid structures. However, in recent studies of nanomaterials, a significantly lower value $q_c \approx 0.03$ was proposed for determination of the melting points of nanosized samples, e.g., carbon nanotubes.[21] Moreover, in MD simulations of melting of various nanostructures presented in the literature, the melting points were observed at values close to $q_c \approx 0.03$ (see Table 1 and related references), thus it seems reasonable to use this value as an indicator of thermally induced degradation for $Ti_{n+1}C_n$ nanosheets. Besides the actual value of the Lindemann index, its temperature dependence also provides information about melting of the sample. It is known that at low temperatures the Lindemann index is small and slowly increases in nearly linear manner with the temperature. At the onset of melting, q is expected to switch to nonlinear increase with temperature. Thus, examining the magnitude and critical behavior of the Lindeman index obtained from Eq. (1), it is possible to estimate the melting point of the sample. To further elucidate structural changes, temperature dependences of the

Table I. Approximate values of Lindemann indexes for various nanostructures near their melting points

Type of nanostructure	Lindemann index
Tetrahexahedral platinum nanoparticle[31]	~0.03
Fullerenol cluster $(C_{60}(OH)_{24})_7$[32]	~0.05
Gold nanorods[33]	0.03–0.013
Cu nanoparticles[34]	~0.25
Gold nanostructures[35]	0.02–0.07
Co clusters[36]	~0.03
Pt–Au nanoparticles with core–shell structure[20]	0.03–0.2
Carbon nanotubes[21]	~0.03

https://doi.org/10.1557/mrc.2019.2 Published online by Cambridge University Press

potential energy and RDF below and above the thermal degradation temperature were also calculated.

Results and discussion

The results of MD simulations are presented in Figs. 2–5. Figure 2 presents the temperature dependence of Lindeman indexes (Fig. 2a) and averaged potential energy (Fig. 2b) for Ti_2C, Ti_3C_2, and Ti_3C_4 samples, calculated from atomistic configurations. As follows from the figure, Lindeman index q exceeds the critical value $q_c = 0.03$ at approximately 1050, 1500, and 1700 K for Ti_2C, Ti_3C_2, and Ti_3C_4 respectively. These temperatures correspond to abrupt changes in $q(T)$ dependencies from slow to very fast growth, which further confirms the thermally induced degradation processes. It is worth noting that the corresponding degradation temperatures increase with the thickness of the MXene samples. Temperature dependencies of the average potential energy calculated around the degradation points (Fig. 2b) also exhibit behavior typical for the melting process with the regions of slow and rapid growth prior to phase transition that results in slowdown of the potential energy growth. Similar trends in potential energy versus temperature have been observed in various MD simulations of the melting processes of other nanostructures.[2,20,21]

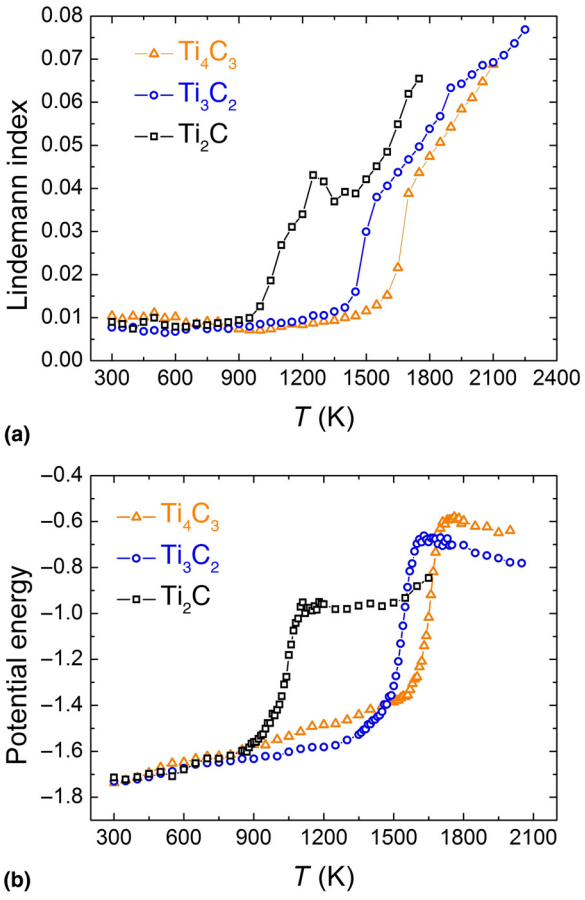


Figure 2. Temperature dependencies of Lindeman index (a) and average potential energy (b) for 2D Ti_2C, Ti_3C_2, and Ti_3C_4.

Snapshots of the systems at two different temperatures (right before the degradation starts and at the point when the degradation is clearly visible), indicating the changes in the atomic structure due to transition from crystal to amorphous configurations are shown in Fig. 3. The top panel represents clearly visible long-range ordered crystal structures of all three MXene samples at the temperatures below the onset of thermal degradation. Snapshots in the bottom panel, taken at higher temperatures, reveal local regions of the amorphous phases, indicating the thermal degradation process.

Top and side views of the atomistic configurations of the samples at maximum simulated temperatures are shown in Fig. 4. As can be seen from the figure, after complete MXene degradation most of the carbon atoms have been vaporized from the samples and move around freely in the simulation box. Titanium atoms tend to form continuous (due to periodic boundary conditions in the *xy* plane) rod-shaped nanostructures for Ti_2C and Ti_3C_2, while for Ti_4C_3 sample Ti atoms largely retain the original shape of a rectangular sheet without voids. This difference may be explained by a larger thickness of Ti_4C_3 sample. Another reason may be due to a greater number of the particles involved in simulations in case of Ti_3C_4, which need more time to re-arrange into a more stable configuration. The fact that carbon atoms do not form any particular structure after the structure degradation, whereas titanium atoms tend to arrange into a kind of a structure, is most likely related to the form of interatomic potentials for carbon and titanium used in our simulations and may be an artifact. Whereas titanium atoms, described by embedded atom method potential, exhibit typical metallic behavior forming nanoparticle-like amorphous structures, carbon atoms interact with titanium and with each other through simple Lennard-Jones potential and thus do not form any specific configurations.

It is important to note that a recent MD simulation with ReaxFF[26] showed that Ti and C atoms in Ti_3C_2 MXene rearrange into cubic titanium carbide TiC at 1500 K in vacuum. As we used simpler approach that does not capture chemical bonding, we only observed the thermal degradation of 2D Ti_3C_2 sample at approximately the same temperature of 1500 K instead of transition to TiC carbide. Thus our approach correctly reproduces the resistance of the 2D Ti_3C_2 MXene structure to heating until the point where the samples no longer maintain planar 2D configuration. At the same time, thermal degradation temperatures for Ti_2C and Ti_4C_3 MXenes obtained in this work are respectively lower (1050 K) and higher (1700 K) than the transition temperature of Ti_3C_2 into cubic TiC reported in Ref. 26. This may be due to the inaccuracy of the used approach or due to the size effects, as Ti_2C and Ti_4C_3 are relatively thinner and thicker, correspondingly, than Ti_3C_2.

For quantitative characterization of the atomic configurations, we calculate RDF at initial and maximal simulated temperatures (Fig. 5). RDF for initial MXene samples (blue lines in

https://doi.org/10.1557/mrc.2019.2 Published online by Cambridge University Press

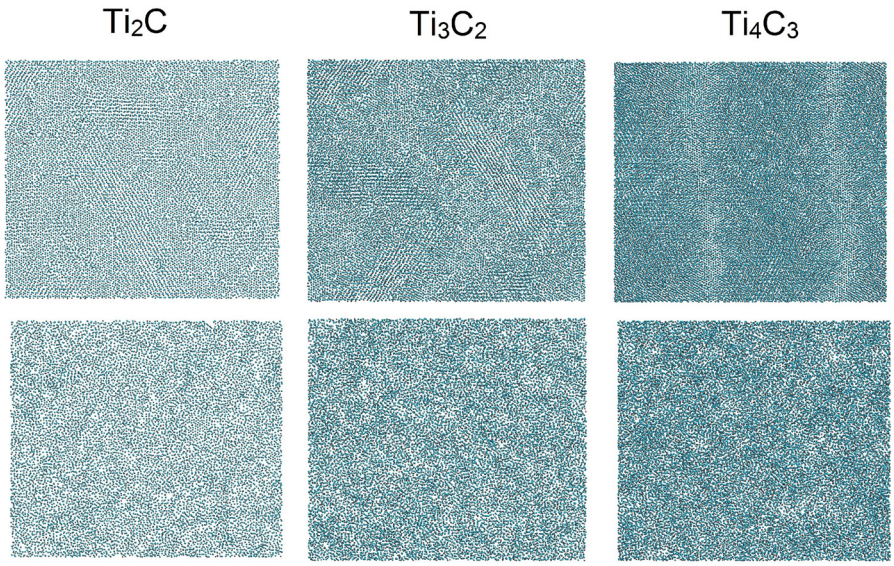


Figure 3. Top view of typical atomistic configurations of 2D Ti_2C, Ti_3C_2, and Ti_3C_4 during heating. Top and bottom panels show the samples with crystal (lower temperature) and amorphous (higher temperature) structures respectively. Corresponding temperatures of the samples (top and bottom snapshots) are 1000 and 1120 K for Ti_2C, 1450 and 1650 K for Ti_3C_2, and 1650 and 1710 K for Ti_3C_4.

the figure) have the shape typical for crystal structures with clearly visible narrow peaks related to equilibrium interatomic distances, indicative of the long-range ordering. Above the degradation point (orange lines in the figure), the RDF shows only short-range ordered structures. Thus, the RDF data confirm the amorphous structure of the samples at the temperatures above their thermal degradation points.

It is worth mentioning that the melting points of other 2D materials obtained from atomistic simulations have been reported at 4510 K (graphene)[22] and 3700 K (MoS_2)[23] respectively. Thus all examined in this paper MXenes have much lower thermal stability compared to graphene and 2D MoS_2.

In general, to obtain more precise values of melting temperatures from MD simulations, it is critical to use a more accurate force field that reproduces breaking and formation of chemical bonds, depending on the external conditions. Other factors to take into consideration when comparing calculated thermal degradation temperatures to experimental ones are ideal vacuum conditions and the absence of surface functional groups, as well as defects in MXene models in our simulations, whereas experimental results (see e.g., Refs. 18 and 19) are produced

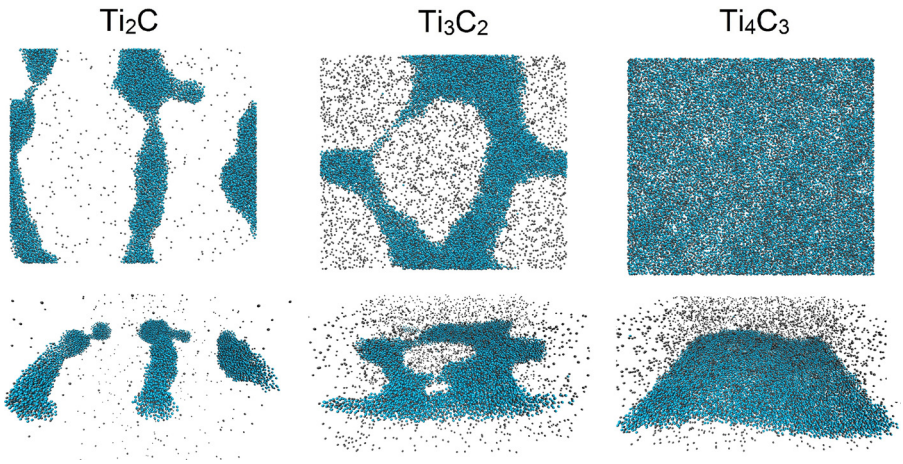


Figure 4. Top (top panel) and side (bottom panel) views of the MXene samples after complete thermal decomposition.

https://doi.org/10.1557/mrc.2019.2 Published online by Cambridge University Press

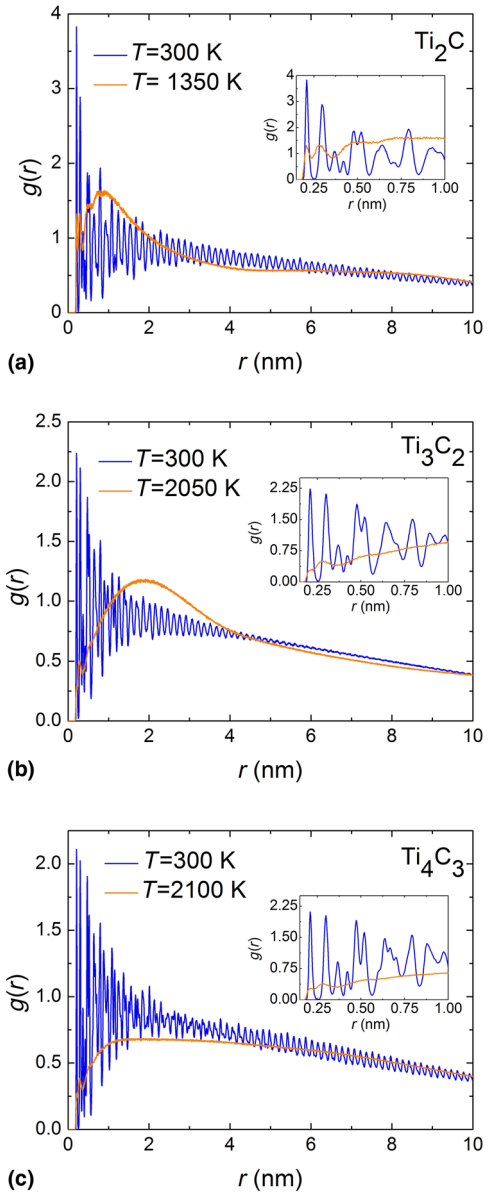


Figure 5. Atomic RDF of the samples at initial and maximal simulated temperature (inner panels show detailed RDF at small distances) for Ti_2C (a), Ti_3C_2 (b), and Ti_3C_4 (c).

with non-ideal vacuum, often under argon or oxygen atmospheres and the real MXene samples are always terminated with surface functional groups and contain structural defects.

Conclusions

The results of classical large-scale MD simulations of the thermal behavior of the 2D titanium carbides were reported. From these data, the approximate values of thermal degradation temperatures 1050, 1500, and 1700 K for Ti_2C, Ti_3C_2, and Ti_3C_4 MXenes have been estimated using the Lindeman index as a melting criterion. The obtained data have been validated by temperature dependencies of the potential energy, snapshots of atomistic configurations, and calculated RDF. Comparison of degradation temperatures of the MXenes with melting points of other typical 2D materials led us to conclude that amorphization and degradation of MXenes (melting) occur at significantly lower temperatures compared to graphene and MoS_2. This needs to be taken into consideration when developing MXenes for nanoelectronics where local heating can be quite severe.

Even though we used simple approach and did not take into account formation of chemical bonds during heating, we believe that our simulations provide a reasonable first-order approximation that can be used in further investigations on the thermodynamic properties of MXenes.

Nomenclature

T	The temperature of the sample
q_i	Lindemann index of an atom i
q	Lindemann index of the sample
q_c	Critical value of the Lindemann index
r_{ij}	The distance between atoms i and j
N	The total number of atoms in the sample

Acknowledgments

VB is grateful to Ministry of Education and Science of Ukraine for financial support (Project No. 0117U003923).

References

1. A. Navrotsky: Energetics at the nanoscale: impacts for geochemistry, the environment, and materials. *MRS Bull.* **41**, 139 (2016).
2. H.A. Alarifi, M. Atis¸, C. Özdog˘an, A. Hu, M. Yavuz, and Y. Zhou: Determination of complete melting and surface premelting points of silver nanoparticles by molecular dynamics simulation. *J. Phys. Chem. C* **117**, 12289 (2013).
3. M. Naguib, M. Kurtoglu, V. Presser, J. Lu, J.J. Niu, M. Heon, L. Hultman, Y. Gogotsi, and M.W. Barsoum: Two-dimensional nanocrystals produced by exfoliation of Ti_3AlC_2. *Adv. Mater.* **23**, 4248 (2011).
4. Y. Dong, S. Chertopalov, K. Maleski, B. Anasori, L. Hu, S. Bhattacharya, A. M. Rao, Y. Gogotsi, V.N. Mochalin, and R. Podila: Saturable absorption in 2D Ti_3C_2 MXene thin films for passive photonic diodes. *Adv. Mater.* **30**, 1705714 (2018).
5. G. Li, K. Kushnir, Y. Dong, S. Chertopalov, A. M. Rao, V.N. Mochalin, R. Podila, and L.V. Titova: Equilibrium and non-equilibrium free carrier dynamics in 2D $Ti_3C_2T_x$ MXenes: THz spectroscopy study. *2D Mater.* **5**, 035043 (2018).
6. S. Chertopalov, and V.N. Mochalin: Environment-sensitive photoresponse of spontaneously partially oxidized Ti_3C_2 MXene thin films. *ACS Nano* **12**, 6109 (2018).
7. D. Er, J. Li, M. Naguib, Y. Gogotsi, and V.B. Shenoy: Ti_3C_2 MXene as a high capacity electrode material for metal (Li, Na, K, Ca) ion batteries. *ACS Appl. Mater. Interfaces* **6**, 11173 (2014).
8. M. Ghidiu, S. Kota, J. Halim, A.W. Sherwood, N. Nedfors, J. Rosen, V. N. Mochalin, and M.W. Barsoum: Alkylammonium cation intercalation into Ti_3C_2 (MXene): effects on properties and ion-exchange capacity estimation. *Chem. Mater.* **29**, 1099 (2017).
9. M. Khazaei, M. Arai, T. Sasaki, C.-Y. Chung, N.S. Venkataramanan, M. Estili, Y. Sakka, and Y. Kawazoe: Novel electronic and magnetic properties of two-dimensional transition metal carbides and nitrides. *Adv. Funct. Mater.* **23**, 2185 (2013).
10. M.R. Lukatskaya, O. Mashtalir, C.E. Ren, Y. Dall'Agnese, P. Rozier, P. L. Taberna, M. Naguib, P. Simon, M.W. Barsoum, and Y. Gogotsi:

https://doi.org/10.1557/mrc.2019.2 Published online by Cambridge University Press

Cation intercalation and high volumetric capacitance of two-dimensional titanium carbide. *Science* **341**, 1502 (2013).
11. M. Naguib, J. Come, B. Dyatkin, V. Presser, P.L. Taberna, P. Simon, M. W. Barsoum, and Y. Gogotsi: MXene: a promising transition metal carbide anode for lithium-ion batteries. *Electrochem. Commun.* **16**, 61 (2012).
12. Y. Dong, S.S.K. Mallineni, K. Maleski, H. Behlow, V.N. Mochalin, A. M. Rao, Y. Gogotsi, and R. Podila: Metallic MXenes: A new family of materials for flexible triboelectric nanogenerators. *Nano Energy* **44**, 103 (2018).
13. A. Lipatov, H. Lu, M. Alhabeb, B. Anasori, A. Gruverman, Y. Gogotsi, and A. Sinitskii: Elastic properties of 2D $Ti_3C_2T_x$; MXene monolayers and bilayers. *Sci. Adv.* **4**, eaat0491 (2018).
14. M. Kurtoglu, M. Naguib, Y. Gogotsi, and M.W. Barsoum: First principles study of two-dimensional early transition metal carbides. *MRS Commun.* **2**, 133 (2012).
15. V.N. Borysiuk, V.N. Mochalin, and Y. Gogotsi: Molecular dynamic study of the mechanical properties of two-dimensional titanium carbides $Ti_{(n+1)}C_{(n)}$ (MXenes). *Nanotechnology* **26**, 265705 (2015).
16. Z. Ning, H. Yu, Y. Sanaz and Z. Mohsen Asle: Superior structural, elastic and electronic properties of 2D titanium nitride MXenes over carbide MXenes: a comprehensive first principles study. *2D Mater.* **5**, 045004 (2018).
17. V.N. Borysiuk, V.N. Mochalin, and Y. Gogotsi: Bending rigidity of two-dimensional titanium carbide (MXene) nanoribbons: a molecular dynamics study. *Comput. Mater. Sci.* **143**, 418 (2018).
18. J. Li, Y. Du, C. Huo, S. Wang, and C. Cui: Thermal stability of two-dimensional Ti_2C nanosheets. *Ceram. Int.* **41**, 2631 (2015).
19. Z. Li, L. Wang, D. Sun, Y. Zhang, B. Liu, Q. Hu, and A. Zhou: Synthesis and thermal stability of two-dimensional carbide MXene Ti_3C_2. *Mater. Sci. Eng. B* **191**, 33 (2015).
20. Z. Yang, X. Yang, and Z. Xu: Molecular dynamics simulation of the melting behavior of Pt–Au nanoparticles with core–shell structure. *J. Phys. Chem. C* **112**, 4937 (2008).
21. K. Zhang, G.M. Stocks, and J. Zhong: Melting and premelting of carbon nanotubes. *Nanotechnology* **18**, 285703 (2007).
22. J.H. Los, K.V. Zakharchenko, M.I. Katsnelson, and A. Fasolino: Melting temperature of graphene. *Phys. Rev. B* **91**, 045415 (2015).
23. S.K. Singh, M. Neek-Amal, S. Costamagna, and F.M. Peeters: Rippling, buckling, and melting of single- and multilayer MoS_2. *Phys. Rev. B* **91**, 014101 (2015).
24. N.C. Osti, M. Naguib, A. Ostadhossein, Y. Xie, P.R.C. Kent, B. Dyatkin, G. Rother, W.T. Heller, A.C.T. van Duin, Y. Gogotsi, and E. Mamontov: Effect of metal ion intercalation on the structure of MXene and water dynamics on its internal surfaces. *ACS Appl. Mater. Interfaces* **8**, 8859 (2016).
25. A.C.T. van Duin, S. Dasgupta, F. Lorant, and W.A. Goddard: ReaxFF: a reactive force field for hydrocarbons. *J. Phys. Chem. A* **105**, 9396 (2001).
26. R. Lotfi, M. Naguib, D.E. Yilmaz, J. Nanda, and A.C.T. van Duin: A comparative study on the oxidation of two-dimensional Ti_3C_2 MXene structures in different environments. *J. Mater. Chem. A* **6**, 12733 (2018).
27. W. Humphrey, A. Dalke, and K. Schulten: VMD: visual molecular dynamics. *J. Mol. Graph. Model.* **14**, 33 (1996).
28. H. Oymak, and F. Erkoc: Titanium coverage on a single-wall carbon nanotube: molecular dynamics simulations. *Chem. Phys.* **300**, 277 (2004).
29. X.W. Zhou, H.N.G. Wadley, R.A. Johnson, D.J. Larson, N. Tabat, A. Cerezo, A.K. Petford-Long, G.D.W. Smith, P.H. Clifton, R.L. Martens, and T.F. Kelly: Atomic scale structure of sputtered metal multilayers. *Acta Mater.* **49**, 4005 (2001).
30. H.J.C. Berendsen, J.P.M. Postma, W.F. Vangunsteren, A. Dinola, and J. R. Haak: Molecular-dynamics with coupling to an external bath. *J. Chem. Phys.* **81**, 3684 (1984).
31. Y.-H. Wen, H. Fang, Z.-Z. Zhu, and S.-G. Sun: A molecular dynamics study of shape transformation and melting of tetrahexahedral platinum nanoparticle. *Chem. Phys. Lett.* **471**, 295 (2009).
32. A. Pia˛tek, A. Dawid, and Z. Gburski: The properties of small fullerenol cluster $(C_{60}(OH)_{24})_7$: computer simulation. *Spectrochim. Acta A* **79**, 819 (2011).
33. R. Essajai, and N. Hassanain: Molecular dynamics study of melting properties of gold nanorods. *J. Mol. Liq.* **261**, 402 (2018).
34. H.H. Kart, H. Yildirim, S. Ozdemir Kart, and T. Çag˘in: Physical properties of Cu nanoparticles: a molecular dynamics study. *Mater. Chem. Phys.* **147**, 204 (2014).
35. R. Essajai, A. Rachadi, E. Feddi, and N. Hassanain: MD simulation-based study on the thermodynamic, structural and liquid properties of gold nanostructures. *Mater. Chem. Phys.* **218**, 116 (2018).
36. S. Lu, J. Zhang, and H. Duan: Melting behaviors of Co_N (N=13, 14, 38, 55, 56) clusters. *Chem. Phys.* **363**, 7 (2009).

https://doi.org/10.1557/mrc.2019.2 Published online by Cambridge University Press